Research Square

Preprints are preliminary reports that have not undergone peer review.
They should not be considered conclusive, used to inform clinical practice,
or referenced by the media as validated information.

Scalable Differentiation of Hematopoietic Progenitor Cells from hiPSCs Using a Bioreactor System

Guirong Kanai-Bai

kanai.guirong.bio.eng@osaka-u.ac.jp

The University of Osaka

Takaya Hataoka

The University of Osaka

Arisa Ito

The University of Osaka

Noriko Yamano-Adachi

The University of Osaka

Takeshi Omasa

The University of Osaka

Article

Keywords: human-induced pluripotent cell, hematopoietic progenitor cell, differentiation, single-use bioreactor, scalability

Posted Date: November 20th, 2025

DOI: https://doi.org/10.21203/rs.3.rs-7975383/v1

License: This work is licensed under a Creative Commons Attribution 4.0 International License.
Read Full License

Additional Declarations: No competing interests reported.

Abstract

A method for scalable and efficient differentiation of hematopoietic progenitor cells (HPCs) from human induced pluripotent stem cells (hiPSCs) represents a pivotal advancement for cell-based therapies targeting cancer, autoimmune disorders, and hematological diseases. Although effective for small-scale production, traditional static culture methods are limited in scalability and reproducibility, necessitating the development of bioreactor-based approaches. In this study, we optimized HPC differentiation from hiPSC lines using a 30-mL stirred suspension bioreactor. The obtained embryoid bodies expanded from ~ 100 μm to 400 μm between days 3 and 13, while their number decreased through fusion. OCT4 expression declined from day 3, followed by transient BRACHYURY and MIXL1 expression, and sequential induction of CD34 from day 7 and CD43 from day 10. Flow cytometry analysis revealed that $CD34^+$ cells peaked at 63.3% on days 9–10, while $CD34^+CD43^+$ cells increased markedly by day 13. The total cell count reached 1.2×10^8 by day 10, yielding 9.7×10^7 $CD34^+$ cells. MM11 hiPSCs differentiated more efficiently than 201B7 hiPSCs, indicating cell line-specific differences. Compared with static culture, this bioreactor system achieved superior yield, uniformity, and scalability. These findings validate the utility of stirred bioreactors for clinical-scale HPC production and provide a foundation for process optimization and translational development.

INTRODUCTION

The clinical potential of human induced pluripotent stem cells (hiPSCs) lies in their ability to generate diverse therapeutically useful cell types [1–5]. Hematopoietic cells, which are progenitors of various immune system cell types, such as macrophages, T cells, and natural killer cells, are particularly relevant for therapeutic applications [6, 7]. These cells form the basis of numerous therapies targeting cancers, autoimmune disorders, infections, and other immune-related conditions. However, the translation of hiPSC-derived HPCs into clinical applications faces significant challenges, primarily due to the differentiation protocol inefficiencies and scalability limitations associated with traditional culture methods [8, 9].

Conventionally, differentiation of hiPSCs into hematopoietic cells has been conducted in static monolayer or aggregate cultures [10–12]. However, these culture systems often rely on media containing animal-derived components. Moreover, static culture modalities have certain limitations, including poor scalability, inadequate oxygen transfer rates, and suboptimal exchange of soluble factors between the cells and their microenvironment [13–15]. These issues pose significant barriers to large-scale clinical applications that require immune cell production.

Recent advances in three-dimensional (3D) cell culture systems, such as spheroids, have demonstrated potential for improving the expansion of hiPSCs and their differentiation into immune cell types [16–19]. Stirred suspension bioreactors (SSBs) represent a practical implementation of such 3D culture systems, providing a robust platform that can overcome the limitations associated with traditional static cultures [17]. By continuously agitating the suspended cells, SSBs ensure uniform nutrient distribution, stable

levels of dissolved oxygen, and controlled hydrodynamic conditions [15]. This type of system facilitates the maintenance of high and uniform cell densities (approximately 10^6–10^7 cells/mL), markedly improving the efficiency of medium and growth factor utilization. Moreover, the high cell density cultures within SSB systems align with the requirements for clinical-scale production (10^8–10^9 cells per patient) [18, 19]. Despite significant advances in hiPSC propagation in bioreactors, guided differentiation of hiPSCs in SSB systems has been relatively limited.

Numerous protocols have been developed for the induction of hiPSC differentiation into immune cell lineages [10–12, 20]. The cells derived using these protocols have been demonstrated to meet critical functional requirements, including the ability to secrete cytokines, such as interleukins, upon stimulation. In studies conducted on preclinical mouse models, the derived cells showed adaptability to tissue-specific environments and anti-leukemic activity [12, 20]. Despite these successes, many of the established differentiation protocols still rely heavily on static culture systems, such as 6-well plates, because of their simplicity and ease of handling in the laboratory. Nevertheless, static culture systems have inherent limitations, primarily arising from poor oxygen distribution and insufficient hydrodynamic mixing [15]. For example, inadequate agitation leads to excessive aggregation of embryoid bodies (EBs), resulting in heterogeneous EB sizes [21]. This size heterogeneity creates hypoxic conditions within larger aggregates, inducing cell death and reducing the overall differentiation efficiency [22]. Such variability not only compromises the experimental consistency but also severely hampers the scalability, with quality control and uniformity becoming increasingly challenging as the production scale increases.

In addition to the issues regarding EB size heterogeneity and hypoxic conditions, static culture protocols are labor-intensive due to the manual processes required, including frequent medium exchanges and harvesting of cells [23]. The protocols also require a large amount of disposable plasticware, which not only substantially elevates the cost but also leads to extensive plastic waste. As differentiation processes scale up, plastic consumption increases proportionally, making sustainable operation economically and environmentally challenging [17, 24–26]. These combined limitations present significant hurdles to scaling differentiation processes and system optimization, ultimately restricting broader clinical applications due to decreased sustainability and economic feasibility.

Bioreactors offer a practical solution to the challenges associated with static cultures by enabling the formation of uniform EBs through controlled stirring and rotation, thereby preventing excessive EB aggregation [17]. The uniformity also ensures a homogeneous distribution of oxygen and nutrients within the EBs, directly enhancing the differentiation efficiency and consistency [25, 27]. Moreover, bioreactors equipped with systems for precise control of pH and dissolved oxygen can optimize the cellular metabolic states and differentiation signaling pathways, creating an optimal environment for both cell proliferation and differentiation. These features make bioreactors a promising platform for scaling hiPSC differentiation protocols while maintaining the reproducibility and product consistency essential for clinical applications [28].

In this study, we investigated the differentiation of hiPSCs into HPCs during culture in a 30-mL SSB and evaluated its advantages over traditional static cultures. Our findings demonstrate that bioreactor-based differentiation enhances EB formation, marker gene expression, and flow cytometric differentiation efficiency, providing a scalable platform for clinical applications.

RESULTS

Progressive increase in EB size with concurrent decrease in EB number during differentiation

Initially, we examined the differentiation of the MM11 cell line, which was established in our laboratory from human peripheral blood mononuclear cells using a Sendai virus vector. Cell differentiation through EB formation was induced in an SSB system, providing scalable and uniform cell culture conditions. Medium exchanges in the system were conducted daily from day 3 post-inoculation, using a protocol adapted from a previous study [29]. In the reported protocol, 80% of the medium was added at the start, followed by 10% supplements on subsequent days, and from day 4 onward, 80% of the medium was exchanged daily. In contrast, we modified this protocol by reducing the initial medium volume to 60% and adding the remaining 20% on days 1 and 2. From day 3 onward, 70% of the medium was exchanged daily. These adjustments shortened the sedimentation time required for medium exchange, reduced the occurrence of oversized EBs, and resulted in markedly improved and more uniform EB formation compared with the original protocol. During the culture, EBs formed as transparent and spherical aggregates, indicating a homogeneous cell distribution and consistent differentiation potential. A representative image taken on day 3 of culture is presented in Fig. 1, showing smooth, uniform, well-defined, and tightly compacted spherical cell aggregates with clear boundaries.

The EBs were imaged on days 3, 7, 10, and 13 to evaluate their growth dynamics. As shown in Fig. 2A, the EB size progressively increased from approximately 100 μm on day 3 to a range of 350–400 μm by day 13. In contrast, the total number of EBs gradually decreased from approximately 17,000 on day 3 to approximately 10,000 by day 13 (Fig. 2B). This decrease in the total number likely arose as smaller EBs merged into larger aggregates, a phenomenon that was clearly observed on day 13 (Fig. 2C). Specifically, as the culture progressed, the increased EB size and density led to more frequent contacts among the EBs, causing them to fuse and contributing directly to the reduction in the total EB count.

Sequential downregulation of pluripotency markers and upregulation of hematopoietic genes during differentiation

Cells were collected on days 3, 7, 10, and 13 for gene expression analysis. Total RNA was extracted and reverse-transcribed into cDNA, followed by RT-qPCR analysis. As shown in Fig. 3A, the expression of OCT4, a pluripotency marker, was significantly decreased from day 3 onward, indicating the loss of pluripotency and the initiation of differentiation. Concurrently, the mesodermal markers BRACHYURY

(Fig. 3B) and MIXL1 (Fig. 3C) were transiently expressed, peaking on day 3 and declining thereafter, suggesting that the cells transitioned from a pluripotent state to the mesodermal lineage and then progressed further along the differentiation pathway.

Expression of CD34 was detected from day 7 onward (Fig. 3D), marking the emergence of HPCs. Furthermore, expression of CD43, a marker of lineage-committed HPCs, was detected at later time points, consistent with its role in a downstream stage of hematopoietic differentiation (Fig. 3E). Collectively, these sequential changes in gene expression indicate a stepwise progression from pluripotency through mesodermal commitment to hematopoietic specification.

Dynamic shifts in CD34 and CD43 expression reveal hematopoietic differentiation kinetics in bioreactor-cultured cells

Flow cytometric analysis was performed to track the differentiation dynamics of MM11 hiPSC-derived HPCs over time (Fig. 4). Fluorescence-activated cell sorting (FACS) analysis of CD34 and CD43 expression in MM11 cells cultured for 7–14 days across three replicate bioreactors revealed a high proportion of $CD34^+$ cells on days 7–10, peaking on days 9 and 10. These observations suggest a predominance of $CD34^+$ cells among the cells during this period. From days 10–14, the proportion of $CD34^+CD43^-$ cells decreased from 60.5% to 55.0% in bioreactor 1, from 59.1% to 40.8% in bioreactor 2, and from 23.2% to 17.4% in bioreactor 3. Notably, the percentage of $CD34^+CD43^+$ double-positive cells peaked on day 13 in all three bioreactors, indicating that the cells were progressing to the next stage of differentiation. Specifically, because CD43 is a marker for more mature cells, the increase in double-positive cells signified the progression of differentiation. However, differences in the proportions of the $CD34^+$ and $CD43^+$ cell populations were observed among the three bioreactors, with bioreactor 3 showing a tendency toward lower numbers of $CD34^+$ cells. These differences may be attributed to variations in the culture conditions or initial cell densities. The tracking of the differentiation process over time revealed that the transition from $CD34^+$ cells to $CD43^+$ cells was a crucial step in the differentiation of MM11 cells. The differences observed among the bioreactors highlight the importance of optimizing the culture conditions, as well as the need for further research to determine the underlying causes of the discrepancies.

To verify the reproducibility of the SSB system, similar culture and differentiation experiments were performed using the 201B7 cell line. The cells were cultured in three different bioreactors for 14 days, and the expression levels of CD34 and CD43 were monitored by flow cytometry on days 10 and 14 (Fig. 5). On day 10, all three bioreactors showed a high proportion of $CD34^+$ cells, indicating the presence of early hematopoietic progenitors, although the percentages of these cells varied. By day 14, marked reductions in the $CD34^+CD43^+$ double-positive population were observed, along with increases in the $CD43^+CD34^-$ population, indicating transition of the cells from early hematopoietic progenitors toward more mature hematopoietic lineages. Notably, bioreactor 1 showed a higher percentage of $CD43^+$ cells on day 14 than the other two bioreactors, indicating that differentiation was potentially more efficient in

this bioreactor. These findings demonstrate the successful differentiation of 201B7 hiPSCs into HPCs in all three bioreactors and further highlight the importance of optimizing the culture conditions for efficient differentiation.

The FACS analyses revealed distinct kinetic characteristics and differentiation efficiencies between the two cell lines during HPC differentiation. The proportion of $CD34^+$ cells peaked on days 9 and 10 and then gradually declined, while the proportion of $CD34^+CD43^+$ double-positive cells significantly increased from day 13, indicating progression to the next differentiation stage. Compared with 201B7 cells, MM11 cells exhibited a higher differentiation rate, with a more rapid decline in $CD34^+CD43^-$ cells and a significantly higher proportion of $CD34^+CD43^+$ double-positive cells after day 10, suggesting a higher hematopoietic differentiation efficiency. Moreover, by day 14, MM11 cells had a lower proportion of $CD34^+CD43^-$ cells and a higher proportion of $CD43^+CD34^-$ cells than 201B7 cells, further supporting the accelerated differentiation. In contrast, 201B7 cells maintained a higher proportion of $CD34^+CD43^-$ cells on day 10, but many of these cells had lost CD34 expression without upregulation of CD43 expression by day 14, resulting in an increased proportion of $CD34^-CD43^-$ double-negative cells. These observations suggest that hematopoietic differentiation may have stalled or that some cells may have deviated toward alternative lineages at the later stage of culture.

The comparison of these two cell lines underscores the importance of evaluating hematopoietic differentiation kinetics across various hiPSC lines to optimize *in vitro* HPC production. Selecting cell lines with inherently higher differentiation efficiency, such as MM11, may enhance the robustness and yield of cell manufacturing strategies for clinical applications.

As both hiPSC lines exhibited relatively high proportions of $CD34^+$ cells during early differentiation, the findings validate the effectiveness of the differentiation protocol and culture conditions used in the SSB system. Under identical conditions, however, the MM11-derived HPCs demonstrated a more advanced hematopoietic differentiation profile than the 201B7-derived HPCs, as evidenced by the earlier and more robust emergence of $CD34^+CD43^+$ double-positive cells. These findings suggest that the observed differences are not attributable to external factors but instead reflect intrinsic variations in the differentiation potential of the two cell lines.

DISCUSSION

This study demonstrates the successful use of an SSB system to facilitate the differentiation of hiPSCs into HPCs. The approach addresses the key limitations of current HPC generation methods, particularly those based on static culture systems, by establishing a scalable and reproducible process for the production of large quantities of functional HPCs.

Compared with static cultures, bioreactor systems offer enhanced control over critical environmental parameters, such as dissolved oxygen, pH, and nutrient distribution. This leads to more uniform EB formation and significantly better differentiation outcomes. Notably, the present study achieved a $CD34^+$

cell yield of approximately 60%, which exceeds the efficiencies typically reported in static culture-based differentiation protocols [10, 21, 30]. These findings underscore the potential of bioreactor systems to support the efficient and clinically relevant production of HPCs from hiPSCs.

The changes in the number and size of EBs observed during culture in the SSB system provide important insights into the dynamics of cell aggregation and differentiation. Initially, many small, well-formed EBs were detected, and these small EBs progressively merged into larger aggregates as the culture progressed. This trend indicates efficient cell aggregation and the onset of differentiation. However, the formation of larger EBs also introduces challenges, such as the development of hypoxic cores, which can negatively affect the cell viability and differentiation efficiency [22].

The present findings are consistent with those in a study conducted by Van Winkle et al. [22], in which a correlation between EB size and limitations in oxygen and nutrient diffusion was noted. The size of EBs plays a critical role in determining the efficiency of oxygen and nutrient diffusion, which in turn influences the differentiation outcomes of hiPSCs. Larger EBs tend to exhibit significant gradients in oxygen and cytokine concentrations, leading to heterogeneous microenvironments that affect cell fate decisions. Therefore, maintaining EBs within an optimal size range is essential to ensure adequate mass transfer and promote consistent and robust differentiation. To address these issues, optimization of the agitation rate to fine-tune the shear stress, along with implementation of perfusion-based culture strategies, may help to maintain the EB size within an optimal range and enhance mass transfer. Such approaches may mitigate the limitations in oxygen and nutrient diffusion in bioreactor culture and ultimately improve the differentiation efficiency of hiPSCs [31].

Gene expression dynamics provide crucial insights into the differentiation process. The rapid decline in OCT4 by day 3, coupled with the peaks in BRACHYURY and MIXL1, observed in the present study indicated early commitment of hiPSCs to the mesodermal lineage, consistent with the findings of a previous study [11]. The subsequent emergence of CD34 expression on day 7 and CD43 on day 10 reflected the transition to hematopoietic lineages. Compared with static culture systems, in which marker expression is often asynchronous and heterogeneous, a bioreactor-based environment can promote more synchronized and robust differentiation. This may be attributed to the controlled and uniform microenvironment provided by the bioreactor, which facilitates consistent lineage progression and improved differentiation efficiency [17].

The flow cytometry analysis on day 10 revealed that approximately 60% of the cells expressed CD34, supporting the effectiveness of the differentiation protocol under the bioreactor conditions used. This yield is comparable to that reported in static 6-well plate cultures, where approximately 49% of the cells were $CD34^+$ by day 6 [10]. While the marker expression levels are similar, the bioreactor system offers a significant advantage in scalability, enabling the expansion of a much larger number of cells due to the greater culture volume and optimized environmental control. Moreover, the capacity of the bioreactor to maintain a uniform oxygen and nutrient distribution contributes to more consistent and reproducible differentiation outcomes. These conditions differ from those in static systems, where localized gradients

and environmental heterogeneity often lead to variability in differentiation efficiency across wells or regions.

The findings of the present study underscore the potential of bioreactor systems to advance the differentiation of HPCs. By addressing the limitations inherent in static culture systems, such as scalability, uniformity, and reproducibility, bioreactor systems provide a robust platform for clinical-scale cell production. In addition, bioreactor systems can support higher cell densities and larger working volumes. For example, the 30-mL bioreactor evaluated in this study achieved a total cell count of 1.2×10^8 cells by day 10, representing a 20-fold increase relative to the initial seeding density. This output meets the requirements for cell therapies, which often demand 10^8–10^9 cells per patient. Studies have also demonstrated the feasibility of scaling SSBs to multi-liter volumes while maintaining both the differentiation efficiency and the product quality [26, 28, 31]. These findings, together with the present results, reinforce the viability of bioreactor-based approaches for clinical translation.

Epigenetic regulation plays a pivotal role in HPC differentiation. Differences in histone modifications, DNA methylation patterns, and chromatin accessibility among cell lines can markedly influence the differentiation efficiency, as demonstrated in recent studies on stem cell epigenetics [32, 33]. The observed variation in the differentiation outcomes between the two hiPSC lines evaluated in this study may be partially attributed to the distinct epigenetic landscapes established during their derivation. However, differences in the two FACS systems used for the two cell lines (FACSMelody™ for MM11 cells and FACSAria™ III for 201B7 cells) may also have influenced the results, as variations in detection sensitivity, laser configurations, and gating strategies can affect the analyzed cell populations. To further elucidate these regulatory mechanisms, future studies integrating single-cell epigenomic profiling and RNA sequencing could provide a more comprehensive understanding of the dynamic gene expressions and chromatin accessibility during differentiation. Such insights would enable refinement of the differentiation protocols, rendering them more tailored and effective. In support of this notion, evidence from prior studies has highlighted the importance of epigenetic factors in guiding efficient differentiation processes [21, 22, 24].

Different bioreactor designs offer unique advantages and trade-offs for HPC differentiation. The SSB system evaluated in this study provided efficient agitation and nutrient distribution, ensuring uniform EB formation and differentiation. Other systems, such as vertical-wheel bioreactors, can minimize shear stress and enhance aggregate homogeneity [31, 34, 35]. Perfusion bioreactors, which enable continuous media exchange and waste removal, offer another promising alternative, particularly for mitigating hypoxia-related issues in larger-scale systems [36–38]. Comparative studies have emphasized the need for further evaluation of bioreactor designs to identify optimal configurations for clinical-scale applications [17, 27, 28].

Despite these advantages of bioreactors, some limitations must be addressed to optimize bioreactor efficacy. One critical challenge is hypoxia, which becomes increasingly pronounced as EBs grow larger and oxygen diffusion is restricted [15]. In the present study, larger EBs exhibited hypoxic cores, which

likely impaired the differentiation efficiency. To mitigate this issue, strategies such as incorporation of microperfusion systems, use of oxygen carriers like perfluorocarbons, and optimization of agitation rates could be considered [39]. Furthermore, the development of real-time monitoring systems for dissolved oxygen levels, coupled with feedback-controlled oxygenation systems, would enable dynamic adjustments to oxygenation and agitation, thereby significantly improving the microenvironment within the bioreactor. These enhancements could lead to better cell viability and differentiation outcomes.

Another challenge is the scalability of the approach, which requires validation in larger bioreactor systems (≥ 10 L) that are commonly used for clinical-scale immune cell production processes, such as CAR-T cell manufacturing. Within these large volumes, the fluid dynamics, shear stresses, and nutrient distributions can differ significantly from those in laboratory-scale formats. Comparative analyses with large-volume systems could provide important benchmarks for overcoming hypoxia-related limitations and refining scale-up strategies [17, 22, 29]. Incorporation of such insights will be essential for the adaptation of bioreactor systems to clinical-scale manufacturing.

To further enhance bioreactor-based differentiation, future efforts should explore advanced bioreactor designs with integrated feedback systems for oxygen and pH control. Investigations of alternative cytokine combinations and timings could further optimize the cell yields. Meanwhile, incorporation of single-cell RNA sequencing may provide deeper insights into the heterogeneity of the differentiated populations, enabling more targeted optimization strategies.

In conclusion, the stirred suspension bioreactor (SSB) system examined in this study demonstrated clear advantages over static cultures in terms of yield, synchronization, and scalability for HPC differentiation. We also achieved high differentiation efficiency using FACS-based separation. Considering that FACS is generally associated with greater cell stress compared with magnetic bead–based approaches more commonly used in clinical settings (e.g., MACS or EasySep), it is reasonable to assume that such softer methods could yield even higher recovery rates. Nevertheless, before any clinical application can be considered, functional analyses of the differentiated cells will be required to confirm their therapeutic relevance. Addressing these challenges would further strengthen the translational potential of this protocol and establish SSB systems as a robust platform for scalable and efficient stem cell-based therapies.

MATERIALS AND METHODS

Cell culture

The 201B7 hiPSC line was obtained from the RIKEN Cell Bank (Tsukuba, Japan). The MM11 hiPSC line was generated in our laboratory by reprogramming human peripheral blood mononuclear cells (Cat# 93000-10M; Lot# 2010113890; FUJIFILM Corporation, Tokyo, Japan) using a CytoTune-iPS 2.0 Reprogramming Kit (Thermo Fisher Scientific, Waltham, MA, USA). Both types of hiPSCs were cultured

on plates coated with iMatrix 511 (0.25 μg/cm^2; #892011; Nippi, Osaka, Japan) in AK02N medium (#AJ100; Ajinomoto, Tokyo, Japan) until they reached 70%–80% confluency.

The cells were then dissociated and transferred to a 30-mL single-use bioreactor (ABLE Biott, Tokyo, Japan), with initial seeding at 2×10^5 cells/mL in 18 mL of medium. Subsequently, 6 mL of Stemline II medium (#S0192; Sigma-Aldrich, St. Louis, MO, USA) was gradually added on days 1 and 2 to facilitate the transition to the differentiation medium, and the culture was agitated at 55 rpm. Medium exchanges were initiated on day 3, with the volume gradually increasing to 30 mL by day 7 to facilitate cell growth and differentiation. At defined time points (days 3, 7, 10, and 14), 5 mL of the culture medium was collected from the bioreactor. For each sample, 2 mL was transferred to a 3×3-cm grid dish (#CS1013; CellSeed Inc., Tokyo, Japan), and 20 random fields were imaged at 4× magnification using a CKX52-22PH inverted microscope (Olympus Corporation, Tokyo, Japan). For the EB diameter and size analyses, 200 EBs were measured using ImageJ software [40].

Hematopoietic cell differentiation of hiPSCs

Hematopoietic differentiation of hiPSCs was induced using a protocol obtained by modifying previously established protocols designed for 6-well plates [30, 41–43]. The detailed differentiation scheme is illustrated in Fig. 6. Differentiation was initiated in a 30-mL single-use bioreactor (ABLE Biott) containing 18 mL of AK02N medium and maintained at 37°C under 5% CO_2 with agitation at 55 rpm.

On days 0–2, AK02N plus Stemline II medium was supplemented with 2 μM GSK-3 inhibitor CHIR99021 (#038-23101; Wako, Osaka, Japan), 20 ng/mL BMP4 (#314-BP-010; R&D Systems, Minneapolis, MN, USA), 40 ng/mL SCF (#255-SC-010; R&D Systems), and 40 ng/mL VEGF (#293-VE-010; R&D Systems).

From days 2–4, the differentiation medium was supplemented with 6 μM ALK5 inhibitor SB431542 (#031-24291; Wako). For days 2–7, 50 ng/mL SCF and 40 ng/mL VEGF were added to the culture medium. For days 7–14, VEGF, SCF, and FLT3L (#308-FK-005; R&D Systems) were added at a final concentration of 50 ng/mL.

RNA extraction and RT-PCR

RNA extraction and RT-PCR
Total RNA extraction and RT-PCR were performed as previously described [44]. Quantitative PCR (qPCR) was conducted using a StepOne Plus Real-Time PCR System (Applied Biosystems, Thermo Fisher Scientific Inc.) in combination with QuantiTect SYBR Green PCR Master Mix (Qiagen, Valencia, CA, USA). The PCR protocol consisted of an initial denaturation step at 95°C for 20 seconds, followed by 30 amplification cycles at 55°C for 30 seconds and 72°C for 35 seconds. A melting curve analysis was conducted from 60°C to 95°C to verify the product specificity.

Relative mRNA expression levels were calculated using standard curves normalized to the GAPDH mRNA expression levels. All measurements were conducted in triplicate for each target gene. The primer sequences were sourced from a previously published study [11].

Flow cytometry and antibodies

Flow cytometric analysis data were acquired using FACSMelody™ and FACSAria™ III systems (BD Biosciences, San Jose, CA, USA) and analyzed with the FlowJo software package (FlowJo LLC, Ashland, OR USA). For all flow cytometric analyses, the cell staining was performed in FACS buffer (0.5% BSA and 2 mM EDTA in PBS) for 30 min on ice, in accordance with the manufacturer's instructions. The antibodies used included CD34-PE (clone 8G12; 348791; BD Biosciences) and CD43-FITC (clone 1G10; 555475; BD Biosciences). Isotype controls, FITC-conjugated mouse IgG2b, and PE-conjugated mouse IgG2a were also obtained from BD Biosciences.

EBs collected from the bioreactor on days 3, 5, 7, 10, 13, and 14 were dissociated using 3×TrypLE Select (A1217701; Thermo Fisher Scientific). The 3×TrypLE solution was prepared by diluting 10×TrypLE Select to the required concentration, and the EBs were incubated in the solution for 10–20 minutes before analysis.

Data availability

The corresponding author can provide the datasets utilized in this study on reasonable request.

Declarations

Competing interests

The authors declare no competing interests.

Funding

This research was supported by the Japan Society for the Promotion of Science (JSPS) through a Grant-in-Aid for Scientific Research (A) (Grant Number: 22H00276), and by collaborative research funding from Merck & Co. Inc., USA.

Author Contribution

G.K. and T.O. designed the study. G.K., T.H., and A.I. conducted the acquisition, analysis, and/or interpretation of data. G.K. wrote the paper. All authors reviewed the manuscript. Figure 1, T.H.; Figure 2, G.K. and T.H.; Figure 3, G.K.; Figure 4, G.K. and T.H.; Figure 5, A.I.; Figure 6, G.K. and T.H.

ACKNOWLEDGMENTS

We thank Alison Sherwin, PhD, from Edanz (https://jp.edanz.com/ac) for editing a draft of this manuscript.

Data Availability

The corresponding author can provide the datasets utilized in this study on reasonable request.

References

1. Takahashi, K. & Yamanaka, S. Induction of Pluripotent Stem Cells from Mouse Embryonic and Adult Fibroblast Cultures by Defined Factors. *Cell* **126**, 663–676 (2006).
2. Nakao, S., Ihara, D., Hasegawa, K. & Kawamura, T. Applications for Induced Pluripotent Stem Cells in Disease Modelling and Drug Development for Heart Diseases. *European Cardiology Review* (2020). (2020). 10.15420/ecr.2019.03
3. Tannenbaum, S. E. & Reubinoff, B. E. Advances in hPSC expansion towards therapeutic entities: A review. *Cell Prolif.* **55**, e13247 (2022).
4. Cerneckis, J., Cai, H. & Shi, Y. Induced pluripotent stem cells (iPSCs): molecular mechanisms of induction and applications. *Signal. Transduct. Target. Therapy*. **9**, 112 (2024).
5. Hoang, D. M. et al. Stem cell-based therapy for human diseases. *Signal. Transduct. Target. Therapy*. **7**, 272 (2022).
6. Kaufman, D. S. Toward clinical therapies using hematopoietic cells derived from human pluripotent stem cells. *Blood* **114**, 3513–3523 (2009).
7. Kim, E. M., Manzar, G. & Zavazava, N. Human iPS cell–derived hematopoietic progenitor cells induce T-cell anergy in in vitro–generated alloreactive CD8 + T cells. *Blood* **121**, 5167–5175 (2013).
8. Jiang, J., Ren, R., Cheng, Y., Li, X. & Zhang, G. Immune cells and RBCs derived from human induced pluripotent stem cells: method, progress, prospective challenges. *Frontiers Cell. Dev. Biology* **11**, (2024).
9. Zimmermannova, O., Caiado, I., Ferreira, A. G. & Pereira, C. F. Cell Fate Reprogramming in the Era of Cancer Immunotherapy. *Frontiers Immunology* **12–2021**, (2021).
10. Zhu, H. & Kaufman, D. S. in *In Vitro Differentiation of T-Cells: Methods and Protocols* (ed. Kaneko, S.) 107–119Springer New York, (2019). 10.1007/978-1-4939-9728-2_12
11. Ng, E. S., Davis, R. P., Azzola, L., Stanley, E. G. & Elefanty, A. G. Forced aggregation of defined numbers of human embryonic stem cells into embryoid bodies fosters robust, reproducible hematopoietic differentiation. *Blood* **106**, 1601–1603 (2005).
12. Iriguchi, S. et al. A clinically applicable and scalable method to regenerate T-cells from iPSCs for off-the-shelf T-cell immunotherapy. *Nat. Commun.* **12**, 430 (2021).

13. Chen, S. et al. In-situ scalable manufacturing of Epstein–Barr virus-specific T-cells using bioreactor with an expandable culture area (BECA). *Sci. Rep.* **12**, 7045 (2022).
14. Selvarajan, V. et al. Piloting a scale-up platform for high-quality human T-cells production. *Frontiers Cell. Dev. Biology* **12–2024**, (2024).
15. Tse, H. M., Gardner, G., Dominguez-Bendala, J. & Fraker, C. A. The Importance of Proper Oxygenation in 3D Culture. *Frontiers Bioeng. Biotechnology* **9–2021**, (2021).
16. Nakagawa, Y. et al. Two differential flows in a bioreactor promoted platelet generation from human pluripotent stem cell–derived megakaryocytes. *Exp. Hematol.* **41**, 742–748 (2013).
17. Kwok, C. K. et al. Scalable expansion of iPSC and their derivatives across multiple lineages. *Reprod. Toxicol.* **112**, 23–35 (2022).
18. Jacobson, E. F. et al. Non-xenogeneic expansion and definitive endoderm differentiation of human pluripotent stem cells in an automated bioreactor. *Biotechnol. Bioeng.* **118**, 979–991 (2021).
19. Kwok, C. K. et al. Scalable stirred suspension culture for the generation of billions of human induced pluripotent stem cells using single-use bioreactors. *J. Tissue Eng. Regen. Med.* **12**, e1076–e1087 (2018).
20. Matsubara, H., Niwa, A., Nakahata, T. & Saito, M. K. Induction of human pluripotent stem cell-derived natural killer cells for immunotherapy under chemically defined conditions. *Biochem. Biophys. Res. Commun.* **515**, 1–8 (2019).
21. Pettinato, G., Wen, X. & Zhang, N. Engineering Strategies for the Formation of Embryoid Bodies from Human Pluripotent Stem Cells. *Stem. Cells. Dev.* **24**, 1595–1609 (2015).
22. Van Winkle, A. P., Gates, I. D. & Kallos, M. S. Mass transfer limitations in embryoid bodies during human embryonic stem cell differentiation. *Cells Tissues Organs.* **196**, 34–47 (2012).
23. Lee, B. et al. Cell Culture Process Scale-Up Challenges for Commercial-Scale Manufacturing of Allogeneic Pluripotent Stem Cell Products. *Bioengineering* 9, (2022).
24. dos Santos, F. F., Andrade, P. Z., da Silva, C. L. & Cabral, J. M. Bioreactor design for clinical-grade expansion of stem cells. *Biotechnol. J.* **8**, 644–654 (2013).
25. Moreira, J. L. et al. Effect of viscosity upon hydrodynamically controlled natural aggregates of animal cells grown in stirred vessels. *Biotechnol. Prog.* **11**, 575–583 (1995).
26. Rodrigues, C. A., Fernandes, T. G., Diogo, M. M., da Silva, C. L. & Cabral, J. M. Stem cell cultivation in bioreactors. *Biotechnol. Adv.* **29**, 815–829 (2011).
27. Fok, E. Y. & Zandstra, P. W. Shear-controlled single-step mouse embryonic stem cell expansion and embryoid body–based differentiation. *Stem Cells*. **23**, 1333–1342 (2005).
28. Jacobson, E. F. et al. Non-xenogeneic expansion and definitive endoderm differentiation of human pluripotent stem cells in an automated bioreactor. *Biotechnol. Bioeng.* **118**, 979–991 (2021).
29. Kwok, C. K. et al. Scalable stirred suspension culture for the generation of billions of human induced pluripotent stem cells using single-use bioreactors. *J. Tissue Eng. Regen. Med.* **12**, e1076–e1087 (2018).

30. Matsubara, H., Niwa, A., Nakahata, T. & Saito, M. K. Induction of human pluripotent stem cell-derived natural killer cells for immunotherapy under chemically defined conditions. *Biochem. Biophys. Res. Commun.* **515**, 1–8 (2019).
31. Borys, B. S. et al. Overcoming bioprocess bottlenecks in the large-scale expansion of high-quality hiPSC aggregates in vertical-wheel stirred suspension bioreactors. *Stem Cell Res. Ther.* **12**, 55 (2021).
32. Wu, H. & Sun, Y. E. Epigenetic Regulation of Stem Cell Differentiation. *Pediatr. Res.* **59**, 21–25 (2006).
33. Zhou, Y. et al. Epigenetic Modifications of Stem Cells. *Circul. Res.* **109**, 1067–1081 (2011).
34. Neto, P. M. et al. Characterization of the Aeration and Hydrodynamics in Vertical-Wheel™ Bioreactors. *Bioengineering* 9, (2022).
35. Dang, T. et al. Computational fluid dynamic characterization of vertical-wheel bioreactors used for effective scale-up of human induced pluripotent stem cell aggregate culture. *Can. J. Chem. Eng.* **99**, 2536–2553 (2021).
36. Braccini, A. et al. Three-Dimensional Perfusion Culture of Human Bone Marrow Cells and Generation of Osteoinductive Grafts. *Stem Cells*. **23**, 1066–1072 (2005).
37. Fong, W. J., Tan, H. L., Choo, A. & Oh, S. K. W. Perfusion cultures of human embryonic stem cells. *Bioprocess Biosyst. Eng.* **27**, 381–387 (2005).
38. Dahlin, R. L., Gershovich, J. G., Kasper, F. K. & Mikos, A. G. Flow Perfusion Co-culture of Human Mesenchymal Stem Cells and Endothelial Cells on Biodegradable Polymer Scaffolds. *Ann. Biomed. Eng.* **42**, 1381–1390 (2014).
39. Chen, G. & Palmer, A. F. Mixtures of hemoglobin-based oxygen carriers and perfluorocarbons exhibit a synergistic effect in oxygenating hepatic hollow fiber bioreactors. *Biotechnol. Bioeng.* **105**, 534–542 (2010).
40. Abramoff, M., Magalhães, P. & Ram, S. J. Image Processing with ImageJ. *Biophotonics Int.* **11**, 36–42 (2003).
41. Robust Highly-Efficient Differentiation of Functional Monocytic Cells from Human Pluripotent Stem Cells under Serum- and Feeder Cell-Free Conditions. *PLOS ONE*. **8**, e59243 (2013).
42. A Novel Serum-Free Monolayer Culture for Orderly Hematopoietic Differentiation of Human Pluripotent Cells via Mesodermal Progenitors. *PLOS ONE* **6**, e22261 (2011).
43. Ohta, R. et al. Laminin-guided highly efficient endothelial commitment from human pluripotent stem cells. *Sci. Rep.* **6**, 35680 (2016).
44. Yamano-Adachi, N. et al. Artificial induction of chromosome aneuploidy in CHO cells alters their function as host cells. *Biotechnol. Bioeng.* **120**, 659–673 (2023).

Figures

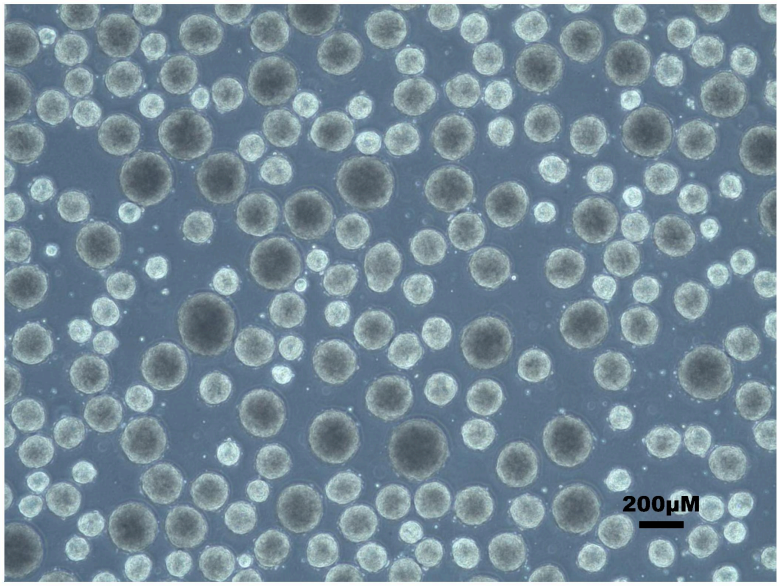


Fig. 1. Image of EBs derived from MM11 hiPSCs on day 3 of culture in the bioreactor. Original magnification: × 10.

Figure 1

See image above for figure legend.

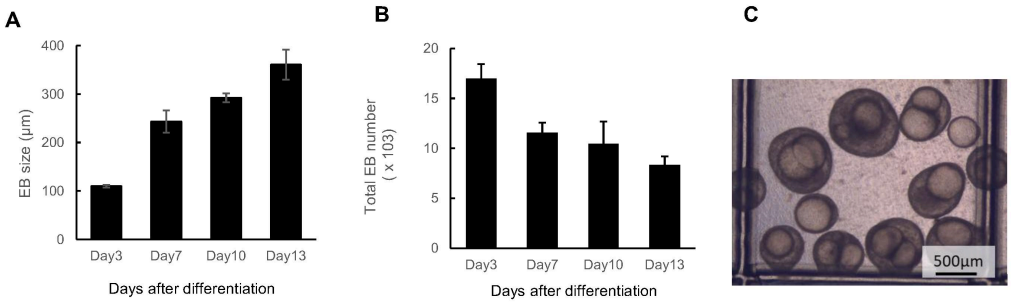


Fig. 2. Differentiation of MM11 hiPSCs to HPC in the bioreactor. (A) Diameters of EBs in the bioreactor on days 3, 7, 10, and 13. A total of 200 EBs were evaluated. Data are shown as mean ± SD. (B) Number of EBs in the bioreactor on days 3, 7, 10, and 13. Data are shown as mean ± SD. (C) Bright-field image of EBs in the bioreactor on day 13. The image shows the fusion of smaller EBs to produce larger aggregates, indicating progressive growth and structural reorganization.

Figure 2

See image above for figure legend.

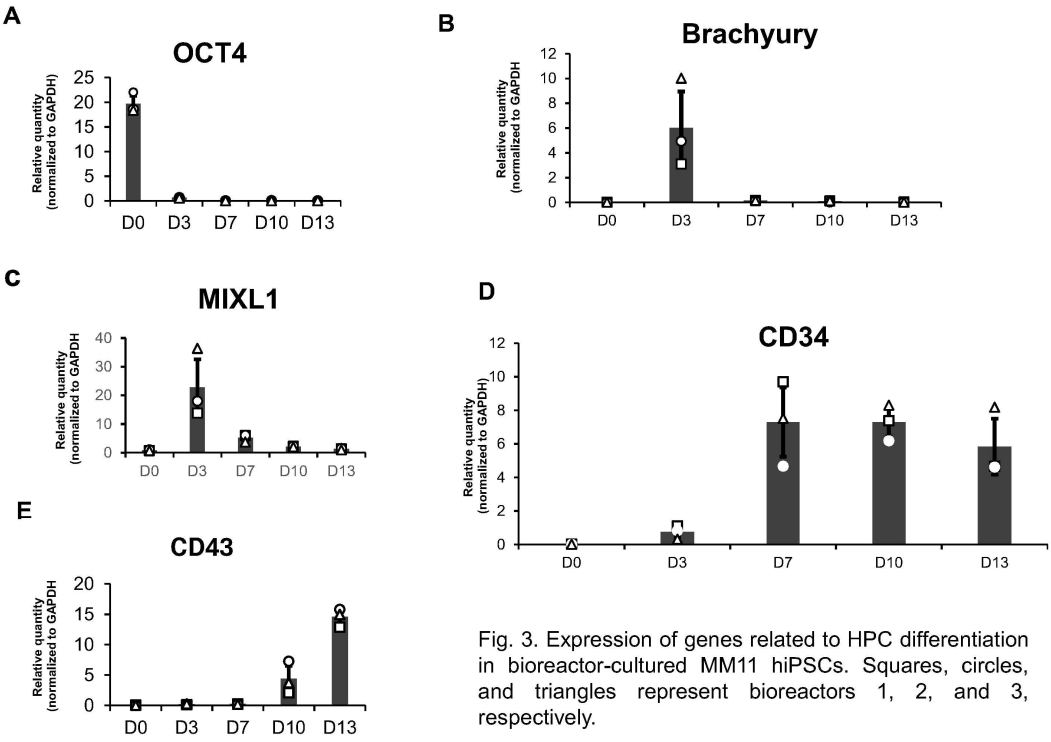


Fig. 3. Expression of genes related to HPC differentiation in bioreactor-cultured MM11 hiPSCs. Squares, circles, and triangles represent bioreactors 1, 2, and 3, respectively.

Figure 3

See image above for figure legend.

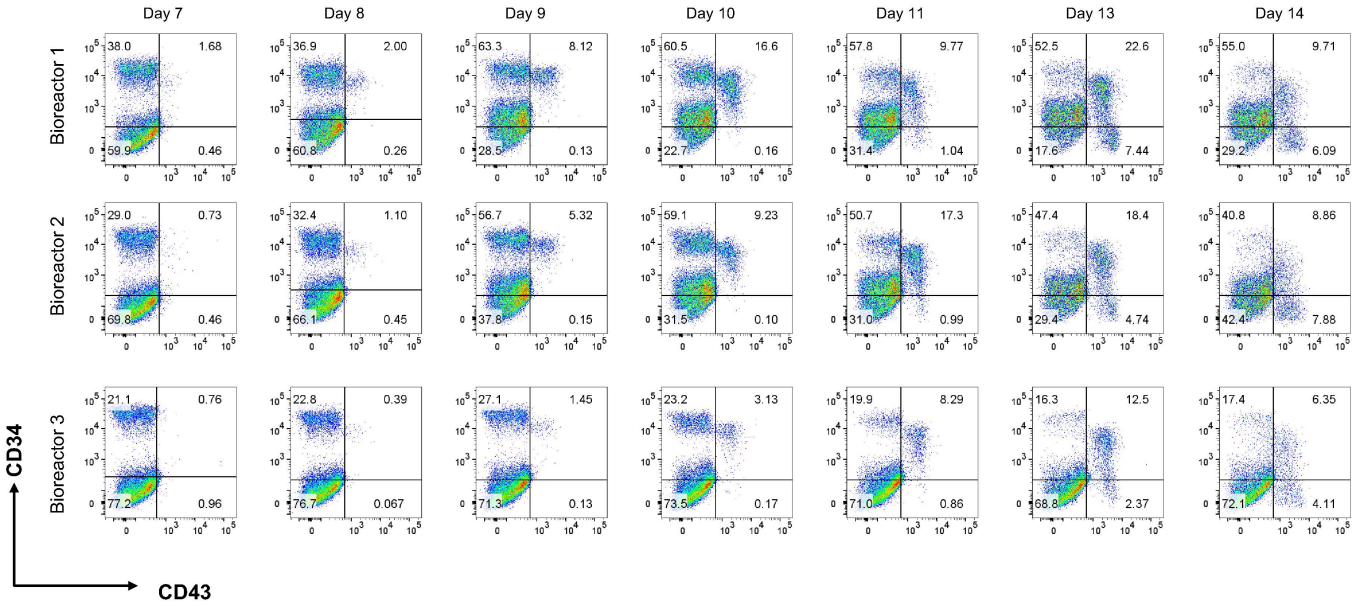


Fig. 4. Representative kinetic flow cytometric analysis demonstrating HPC differentiation of MM11 hiPSCs on days 7–14 in three replicate bioreactors. The examined antigens are indicated on the left side of the figure.

Figure 4

See image above for figure legend.

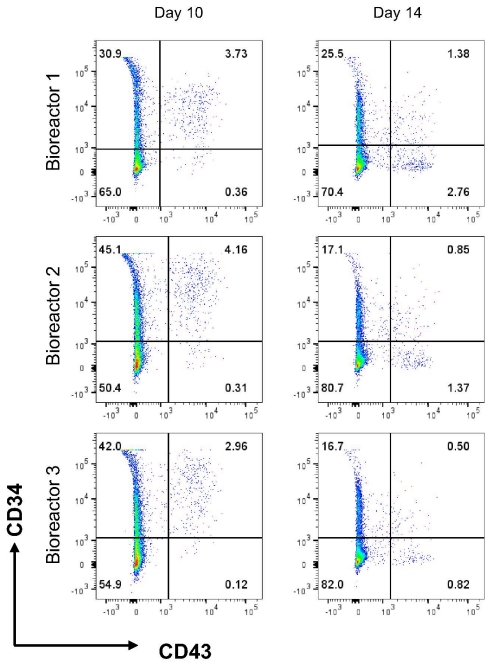


Fig. 5. Representative kinetic flow cytometric analysis demonstrating HPC differentiation from 201B7 cells on days 10 and 14 in three replicate bioreactors. The examined antigens are indicated on the left side of the figure.

Figure 5

See image above for figure legend.

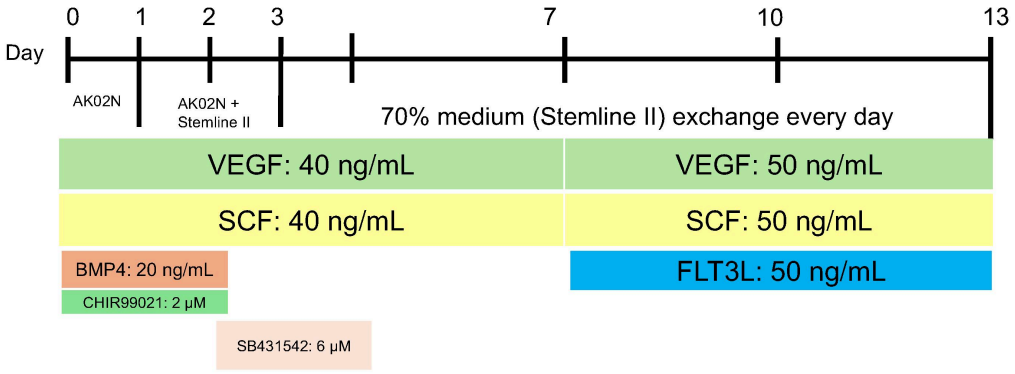


Fig. 6. Schematic diagram showing the induction of hematopoietic differentiation from hiPSCs. EBs were generated from single-cell dissociated hiPSCs proliferated under feeder- and serum-free conditions and induced to differentiate initially into mesodermal cells and later into hematopoietic cells in the presence of CHIR99021, BMP4, SB431542, bFGF, SCF, VEGF, and FLT3L. hiPSCs were cultured in the bioreactor at 2×10^5 hiPSCs/mL with stirring at 55 rpm, using an initial volume of 18 mL in the optimized protocol. In this protocol, a further 6 mL of medium was added on each of days 2 and 3 post-inoculation. Daily medium exchanges of up to 30 mL were performed from day 3 post-inoculation.

Figure 6

See image above for figure legend.